MRI image harmonization using cycle-consistent generative adversarial network

Conference Paper · March 2020

DOI: 10.1117/12.2551301

4 authors, including:

Gourav Modanwal
Case Western Reserve University
13 PUBLICATIONS **72** CITATIONS

SEE PROFILE

Mateusz Buda
Duke University
14 PUBLICATIONS **1,484** CITATIONS

SEE PROFILE

Maciej Mazurowski
Duke University Medical Center
147 PUBLICATIONS **4,124** CITATIONS

SEE PROFILE

MRI Image Harmonization using Cycle-Consistent Generative Adversarial Network

Gourav Modanwal[a], Adithya Vellal[b], Mateusz Buda[a], and Maciej A. Mazurowski[a]

[a]Dept. of Radiology, Duke University, 2424 Erwin Rd., Durham, NC, USA
[b]Dept. of Computer Science, Duke University, 308 Research Dr., Durham, NC, USA

ABSTRACT

Dynamic contrast-enhanced magnetic resonance imaging (DCE-MRI) has proven to be a useful modality for evaluating breast abnormalities found in mammography and performing early disease detection in high-risk patients. However, radiological images generated by various vendors of MRI scanners (e.g., GE Healthcare & Siemens) vary greatly in terms of intensity and other image characteristics such as noise distribution. This is a challenge both for the evaluation of images by radiologists and for the computational analysis of images using radiomics or deep learning. For example, an algorithm trained on a set of images acquired by one MRI scanner may perform poorly on a dataset produced by a different scanner. Therefore, there is an urgent need for image harmonization. Traditional image to image translation algorithms can be used to solve this problem, but they require paired data (i.e., the same object imaged using different scanners). In this study, we utilize a deep learning algorithm that uses unpaired data to solve this problem through a bi-directional translation between MRI images. The proposed method is based on a cycle-consistent adversarial network (CycleGAN) that uses two generator-discriminator pairs. The original CycleGAN struggles in preserving the structure (i.e., breast tissue characteristics and shape) during the translation. To overcome this, we modified the discriminator architecture and forced the penalization based on the structure at the scale of smaller patches. This allows the network to focus more on features pertaining to breast tissue. The results demonstrate that the output images are visually realistic, preserve the structure and harmonize intensity across images from different scanners.

Keywords: MRI, Intensity Harmonization, Medical Image Translation, Deep Learning, CycleGAN

1. INTRODUCTION

Breast cancer is among the world's preeminent causes of death among women.[1] Dynamic contrast-enhanced magnetic resonance imaging (DCE-MRI) is often utilized when evaluating the extent of breast cancer before surgery. However, different MRI scanners use varying parameters, which have been shown to dramatically modify image appearance, quality, and even radiological understanding.[2] Irregularities in the radio-frequency (RF) coil cause intensity fluctuations of the imaged tissue.[3] Within radiomics, where numerous features are extracted for downstream analyses, features obtained from different scanner parameter settings may be incomparable, rendering them useless for classification and prediction tasks. Additionally, deep learning models[4] are also known to struggle with such variability. Computer-assisted diagnostic algorithms trained on a set of images from one scanner model may not generalize to images obtained from another scanner. Having a method for translating between images captured by different vendors with varying parameters of scanner would be highly beneficial. Such an algorithm would make it easy to analyze datasets spanning images from numerous institutions. It would also enhance the generalization of future deep learning models, as models trained on one dataset would be able to perform inference on datasets produced by different scanners.

To overcome this issue, we present an MRI image harmonization algorithm that performs unpaired bidirectional translation between DCE-MRIs generated by different scanners. First, we adapt the standard CycleGAN

Send correspondence to Maciej A. Mazurowski: maciej.mazurowski@duke.edu
Citation: Gourav Modanwal, Adithya Vellal, Mateusz Buda, and Maciej A. Mazurowski "MRI image harmonization using cycle-consistent generative adversarial network", Proc. SPIE 11314, Medical Imaging 2020: Computer-Aided Diagnosis, 1131413 (16 March 2020); https://doi.org/10.1117/12.2551301

for the harmonization task and note its inability to maintain the shape of the breast as well as the tissue structures within the breast. We then propose and evaluate a technical solution to this issue: a modified discriminator architecture capable of preserving both the breast shape and the dense tissue structures. We then evaluate our proposed improvement both quantitatively and qualitatively, and we conclude by highlighting how our algorithm can aid in the creation of larger and richer data-sets for radiomics analyses.

2. METHODS

2.1 Dataset and Preprocessing

In this work, we used DCE MRI images (axial plane) captured using GE Healthcare (GE) and Siemens (SE) scanners with a 1.5 Tesla field strength. Our database consisted of 124 subjects in total. Out of this, 77 subjects were imaged with a GE scanner and the other 47 were imaged with an SE scanner. We used the middle 50% of 2D axial slices from every 3D image (each volume was initially composed of 160+ slices). The top 1% of pixel values were truncated, and all were set to 255, while the remaining pixels were scaled linearly to the range 0-255. We trained the algorithm with a training set of 5045 GE slices and 2776 SE slices. Meanwhile, our test set included 1563 GE slices and 843 SE slices, and our validation set has 173 GE slices and 93 SE slices.

2.2 Standard CycleGAN

The CycleGAN architecture, as proposed by Zhu et al.,[5] contains two generator-discriminator pairs (G_1, D_1, G_2, D_2). They are trained in an adversarial paradigm in which G_1 competes with D_1 and G_2 competes with D_2 as shown in Figure 1. Generator G_1 takes a sample I_1 from $P_{data}(GE)$ as input and generates an output image that belongs to $P_{data}(SE)$. Similarly, generator G_2 takes a sample I_2 from $P_{data}(SE)$ as input and outputs an image that belongs to $P_{data}(GE)$. Meanwhile, D_1 discriminates between generated image $G_1(I_1)$ and the target image I_2, while G_1 attempts to fool the discriminator into an incorrect classification by enhancing the transformed image. The generator-discriminator pair (G_2, D_2) behaves in an analogous manner.

The generator architecture is adapted from Johnson et al.[6] It is a fully convolutional neural network, composed of an encoder, transformer, and decoder. The encoder performs fully convolutional downsampling. The transformer block uses residual convolutional blocks to modify the latent representation. Lastly, the decoder performs fully convolutional upsampling. The output volume matches the input volume in both spatial dimensions as well as depth.

The discriminator is a PatchGAN,[7] a fully convolutional network that takes overlapping patches as inputs instead of processing the entire image at once. The PatchGAN outputs a classification matrix which specifies whether each patch is either real or fake. A standard PatchGAN has 70×70 field of view (FOV), or patch

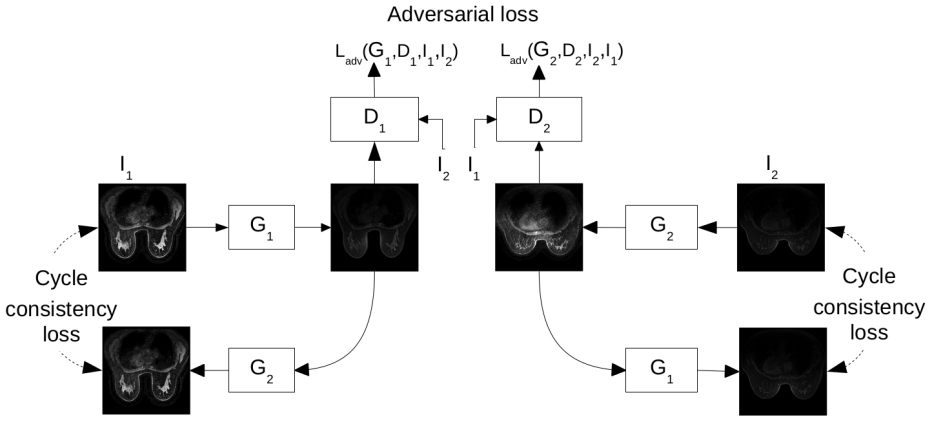

Figure 1. CycleGAN network configuration.

size. We experimented with varying FOV and modified the discriminator architectures. The results obtained are discussed in Section 3.

The CycleGAN is trained using a min-max optimization process, which involves two loss functions, namely adversarial loss (L_{adv}) and cycle consistency loss (L_{cyc}). The adversarial loss aims to make it appear as if the generated images belong to the same data distribution as the target image. Additionally, by enforcing the generators G_1 and G_2 be inverses i.e. $(G_2(G_1(I_1)) \approx I_1$ and $(G_1(G_2(I_2)) \approx I_2)$, L_{cyc} guarantees that the translated image appears similar to the input image. The formulas for L_{adv} and L_{cyc} are provided below.

$$L_{adv}(G_1, D_1, I_1, I_2) = \mathbb{E}_{I_2 \sim P_{data}(SE)} \left[(D_1(I_2) - 1)^2\right] + \mathbb{E}_{I_1 \sim P_{data}(GE)} \left[(D_1(G_1(I_1)))^2\right] \tag{1}$$

$$L_{adv}(G_2, D_2, I_2, I_1) = \mathbb{E}_{I_1 \sim P_{data}(GE)} \left[(D_2(I_1) - 1)^2\right] + \mathbb{E}_{I_2 \sim P_{data}(SE)} \left[(D_2(G_2(I_2)))^2\right] \tag{2}$$

$$L_{cyc}(G_1, G_2) = \mathbb{E}_{I_1 \sim P_{data}(GE)} \left[\|G_2(G_1(I_1)) - I_1\|_1\right] + \mathbb{E}_{I_2 \sim P_{data}(SE)} \left[\|G_1(G_2(I_2)) - I_2\|_1\right] \tag{3}$$

This leads to our full objective, with the weighing factor λ_{cyc}:

$$L(G_1, G_2, D_1, D_2) = L_{adv}(G_1, D_1, I_1, I_2) + L_{adv}(G_2, D_2, I_2, I_1) + \lambda_{cyc} * L_{cyc}(G_1, G_2) \tag{4}$$

Taking Mao et al.'s, 2017[8] suggestion, we use mean squared error (MSE) to train our CycleGAN networks instead of cross-entropy, leading to a more stable training process and a higher quality of generated images. Additionally, providing the discriminator with a buffer of the 50 most recently generated images minimizes model oscillation. Adam optimizer with $l_r = 0.002$ and $\beta_1 = 0.5$, $\beta_2 = 0.999$ is used during training.

2.3 Modified Discriminator

We evaluated the performance of varying FOV in the discriminator architecture. Based on our results, we proposed a modified discriminator architecture with the ability to prioritize the breast tissue characteristic. The modified architecture with smaller FOV is shown in Figure 2. The architecture of the modified discriminator processes smaller (34×34) patches of the input image rather than the 70×70 patches of the original PatchGAN. The change in FOV enforces the generation of sharp, high-frequency details that are essential for the successful preservation of the overall breast structure as well as the dense tissue regions within the breast.

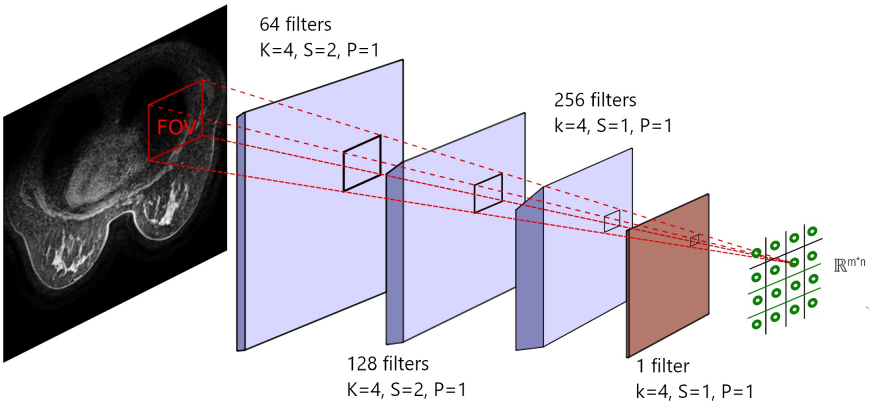

Figure 2. Discriminator architecture.

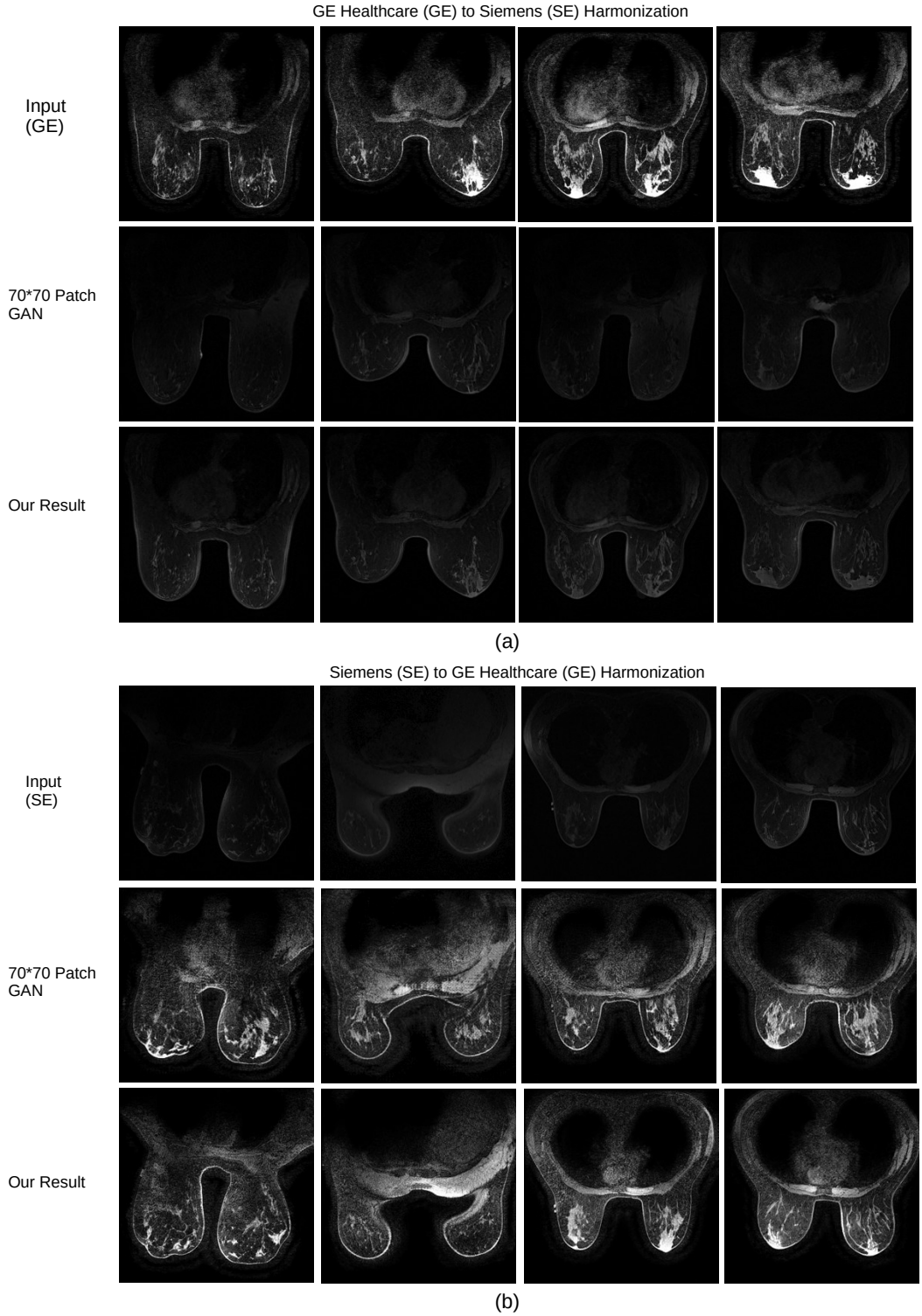

Figure 3. Proposed Image Harmonization Results (a) GE Healthcare to Siemens (b) Siemens to GE Healthcare.

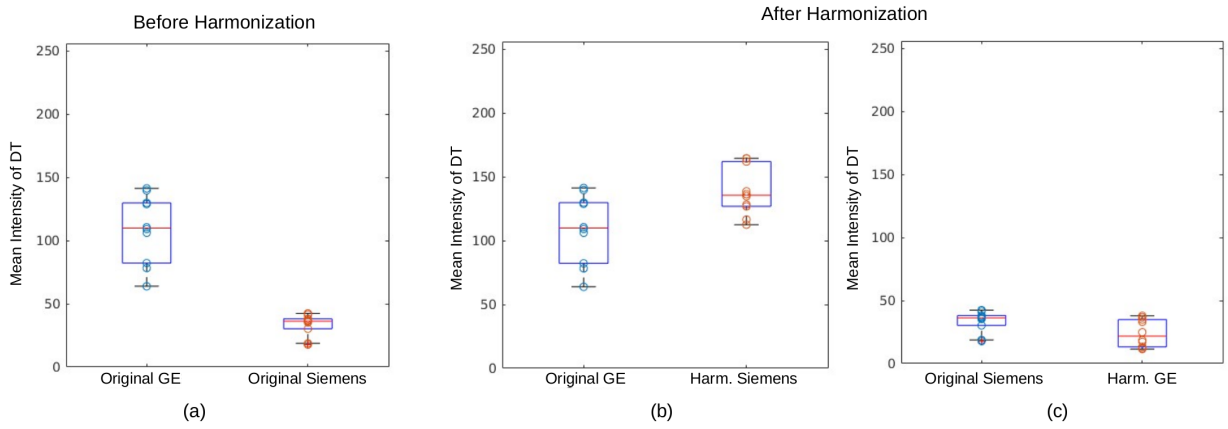

Figure 4. Illustration of mean intensity value distribution in dense tissues (a) before harmonization (b, c) after harmonization.

3. RESULTS

We evaluated the success of the proposed approach, both quantitatively and qualitatively. To assess the performance of the intensity harmonization, we did manual annotation of the dense tissue (10 cases) and used these annotations to calculate mean intensity values before and after harmonization. Due to varying scanner parameters, the mean intensity value of dense tissue is different between the GE and Siemens MRIs; the expectation is that after harmonization, they should be alike. To test our algorithm qualitatively, we did a visual inspection of whether the overall breast shape and dense tissue regions' shapes were altered or not.

The result of the proposed image harmonization from GE Healthcare (GE) to Siemens (SE) and from Siemens (SE) to GE Healthcare (GE) is shown in Figure 3. It can be observed that the 70×70 PatchGAN discriminator often alters both overall breast shape and dense tissue regions. The proposed modification in the discriminator architecture retains the characteristics of the breast tissue as well as the holistic shape of the breast. Figure 4(a) depicts the mean intensity value distributions of dense tissue regions in both GE and Siemens prior to harmonization. Figure 4(b) demonstrates that the mean intensity value distributions of the original GE and harmonized Siemens images are comparable. A similar conclusion can be reached for the original Siemens and harmonized GE case after examining Figure 4(c).

4. CONCLUSION

In this study, we have demonstrated that the generative adversarial network (GAN) paradigm can be used to perform harmonization of DCE-MRIs produced by GE Healthcare & Siemens scanners. The proposed method not only performs intensity harmonization, but also learns the pattern of noise distribution. The experiments in this study show that the standard CycleGAN algorithm, when applied to the task of MRI image harmonization, can produce the desired intensity but struggles to maintain holistic breast shape as well as dense tissue structure. In order to mitigate this, we proposed a modified discriminator architecture with a smaller field of view to emphasize more on features specific to breast tissue and shape. Our experiments indicate that this solution was successful in achieving the desired properties. The output images are visually realistic, preserve the structure (i.e., breast tissue characteristics and shape) and harmonize intensity across images from different scanners.

It is important to note that our study had a few limitations. Currently, our proposed method can only translate 2D MRI slices. However, if computational resources are available as well as time is devoted to network architecture design and parameter optimization, these methods can be extended to $3D$ volumes. In our future research, we intend to extend the network models to $3D$ volumes.

To summarize, we introduced a CycleGAN-based framework for harmonizing breast MRIs. To combat some of the challenges we faced while applying this framework, we developed a technical innovation that enabled our

system to succeed at the task of breast MRI harmonization. While this methodology was only tested with breast MRIs, it can be naturally extended to other medical imaging pipelines that require unpaired harmonization.

APPENDIX A. DISCRIMINATOR ARCHITECTURE DETAILS

This section presents discriminator architectures with different field of view. All specified models use a final convolution to generate an $m \times m$ output. InstanceNorm was only used in the first convolutional layer of both architectures, and LeakyRELU with slope 0.2 was used as the activation function.

Table 1. Discriminator architecture (70×70)

Layer	Input Channel	Output Channel	Filter Size (k)	Stride (S)	Activation
Convolution	1	64	4×4	2	Leaky ReLU
Convolution	64	128	4×4	2	Leaky ReLU
Convolution	128	256	4×4	2	Leaky ReLU
Convolution	256	512	4×4	1	Leaky ReLU
Convolution	512	1	4×4	1	-

Table 2. Discriminator architecture (34×34)

Layer	Input Channel	Output Channel	Filter Size (k)	Stride (S)	Activation
Convolution	1	64	4×4	2	Leaky ReLU
Convolution	64	128	4×4	2	Leaky ReLU
Convolution	128	256	4×4	1	Leaky ReLU
Convolution	256	1	4×4	1	-

REFERENCES

[1] American Cancer Society, "Breast Cancer Facts & Figures 2019-2020," (American Cancer Society, Inc. 2019).

[2] Saha, A., Yu, X., Sahoo, D., and Mazurowski, M. A., "Effects of MRI scanner parameters on breast cancer radiomics," *Expert systems with applications* **87**, 384–391 (2017).

[3] Roy, S., Carass, A., Bazin, P.-L., and Prince, J. L., "Intensity inhomogeneity correction of magnetic resonance images using patches," in [*Medical Imaging 2011: Image Processing*], **7962**, International Society for Optics and Photonics (2011).

[4] AlBadawy, E. A., Saha, A., and Mazurowski, M. A., "Deep learning for segmentation of brain tumors: Impact of cross-institutional training and testing," *Medical physics* **45**(3), 1150–1158 (2018).

[5] Zhu, J.-Y., Park, T., Isola, P., and Efros, A. A., "Unpaired image-to-image translation using cycle-consistent adversarial networks," in [*Proceedings of the IEEE International Conference on Computer Vision (ICCV)*], (Oct 2017).

[6] Johnson, J., Alahi, A., and Li, F., "Perceptual losses for real-time style transfer and super-resolution," *CoRR* **abs/1603.08155** (2016).

[7] Isola, P., Zhu, J.-Y., Zhou, T., and Efros, A. A., "Image-to-image translation with conditional adversarial networks," in [*Proceedings of the IEEE conference on computer vision and pattern recognition*], 1125–1134 (2017).

[8] Mao, X., Li, Q., Xie, H., Lau, R. Y., Wang, Z., and Paul Smolley, S., "Least squares generative adversarial networks," in [*Proceedings of the IEEE International Conference on Computer Vision (ICCV)*], (Oct 2017).